JOURNAL OF GEOPHYSICAL RESEARCH, VOL. 103, NO. 10, PAGES 23,653–23,660, OCTOBER 1, 1998

A simple simulation of a plasma void: Applications to Wind observations of the lunar wake

W. M. Farrell and M. L. Kaiser
Laboratory for Extraterrestrial Physics, NASA Goddard Space Flight Center, Greenbelt, Maryland

J. T. Steinberg
Center for Space Research, Massachusetts Institute of Technology, Cambridge

S. D. Bale
Space Science Laboratory, University of California, Berkeley

Abstract. Previously, the formation of the lunar wake was considered from a magnetohydrodynamic perspective. However, recent Wind particle and field observations suggest the lunar wake may be formed by kinetic processes: those microphysical processes not considered in an MHD formalism. Unfortunately, a full multidimensional and self-consistent kinetic simulation of the lunar wake is beyond current means. However, some elements of the kinetic structure can be simulated via a simple one-dimensional electrostatic particle-in-cell simulation. We present a self-consistent simulation of a cross-sectional element of a plasma void. Essentially, wakeward directed ion beams are formed at the flanks of the simulated void, consistent with the Wind observations of counterstreaming ion beams in the wake region. These wakeward directed beams are generated by ambipolar electric fields formed at the wake edges. Other structures observed by Wind are also seen in the simulation, including an electrostatically turbulent central wake region that causes the wake to fill-in and a rarefaction wave emanating outward from the wake.

1. Introduction

The Wind spacecraft was launched in November 1994 as part of the Global Geospace Science (GGS) fleet, and thereafter followed a double-lunar swingby orbit to allow for long periods of solar wind study. This orbit was primarily designed for lunar gravitational assist to boost the spacecraft to increasing perigee. However, the moon also became a target of opportunity for scientific study of the solar wind interaction with a nonmagnetic body, now with modern instrumentation [*Ogilvie et al.*, 1996; *Owen et al.*, 1996; *Bosqued et al.*, 1996; *Kellogg et al.*, 1996; *Farrell et al.*, 1996, 1997; *Bale et al.*, 1997; *Bale*, 1997].

Preceding studies occurring in the late 1960s and early 1970s tended to emphasize the magnetohydrodynamic nature of the moon [*Spreiter et al.*, 1970]: a picture dominated by a plasma void that quickly filled in approximately 2–3 Lunar radii downstream of the body. A trailing shock was then suggested to be present further down the tail, as indicated by Figure 17 of *Spreiter et al.* [1970]. Unfortunately, these early investigations had relatively low resolution magnetometers, and did not have simultaneous particle distribution and plasma wave measurements. As a consequence, there was an understandable deemphasis on plasma kinetic effects since the fundamental measurements of such processes where not available. However, some debate over an MHD versus particle/kinetic lunar wake did occur, as described in the introduction of *Spreiter et al.* [1970]. Unfortunately, high-resolution particle and electric wave measurements were unavailable to aid in their discussion.

Paper number 97JA03717.
0148-0227/98/97JA-03717$09.00

In contrast, the Wind spacecraft has made a dozen passes near the lunar wake, now with advanced magnetic field (MFI) [*Lepping et al.*, 1995], particle (SWE) [*Ogilvie et al.*, 1995] and plasma wave (WAVES) [*Bougeret et al.*, 1995] instruments all operating simultaneously in the region. As a consequence, it now appears that the activity surrounding the lunar absorption of solar wind is far more kinetic in nature than previously discussed. Even though the scale size is appropriate for an MHD interactions, kinetic instabilities appear to play a dominate role. The evidence for this shift in paradigm includes the following:

1. A wake-related ion and electron density dropout of nearly a factor of 100 below ambient levels was observed 7 R_L downstream from the body [*Bosqued et al.*, 1996; *Ogilvie et al.*, 1996]. The observation indicated that the wake density dropout extends further downstream than predicted based on the magnetosonic approximations and suggests some other underlying physical process is occurring.

2. Counterstreaming ion beams originating from each of the wake flanks were discovered to be in the central lunar wake region [*Ogilvie et al.*, 1996]. The beam energy appears to be consistent with a simple analytical model of plasma expansion into a void via ambipolar processes [*Ogilvie et al.*, 1996; *Samir et al.*, 1983]. Wake-related ion beams have been detected downstream by Wind as far as 23 R_L (J. T. Steinberg, private communication, 1997).

3. Broadband electrostatic noise was also observed in the central wake [*Kellogg et al.*, 1996; *Bale et al.*, 1997] simultaneously with the counterstreaming ions in the region [*Ogilvie et al.*, 1996]. The associated electrostatic instability was suggested to slow down or "brake" the incoming ion flows for depositing in the region. The instability is thus a kinetic mechanism for ion replenishment in the wake [*Farrell et al.*, 1997].

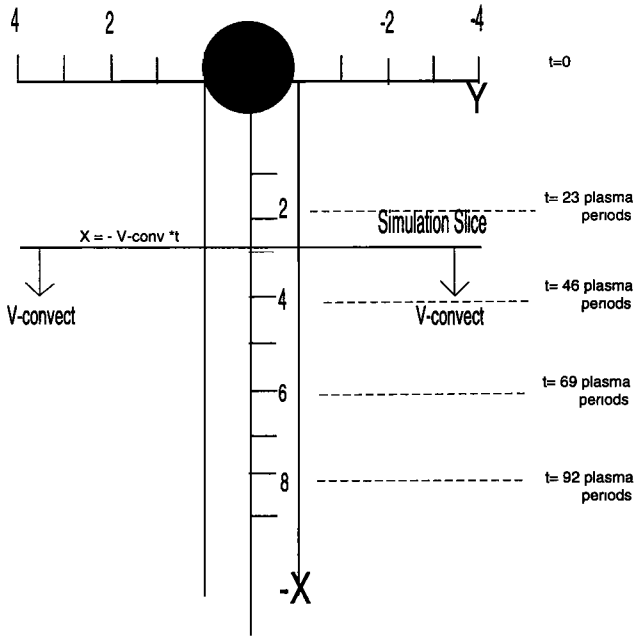

Figure 1. Illustration of simulation geometry.

4. On field lines connected to the wake, there appears to be outflowing electrons and enhanced plasma wave activity in many modes [*Farrell et al.*, 1996; *Bale et al.*, 1997; *Bale*, 1997]. Such upstream disturbances (appearing as "electron wings") occur at a flaring angle much greater than any Alfvenic disturbance predicted via MHD and is considered kinetic in nature.

In order to explain the ion beam formation in the central lunar wake region, *Ogilvie et al.* [1996] presented a one-dimension analytical model of plasma expansion in to a vacuum [see *Samir et al.*, 1983, and references therein]. Solving for the fluid motion of the ions and Maxwellian electrons, they found that ion beam formation will occur, with beam propagation directed into the wake at velocities exceeding the ion thermal speed. Also, a density rarefaction wave will be emitted outward from the wake as ions are drawn from the surrounding plasma into the void. These analytical results are consistent with the Wind observations. We present results from a simple one-dimensional (1-D) kinetic simulation of the plasma expansion process into a void that expands upon and advances the *Ogilvie et al.* [1996] analytical model. The results of the simulation will then be compared to observations. As we shall demonstrate, the kinetic aspects of the wake dynamics can create rather unusual and unexpected structures.

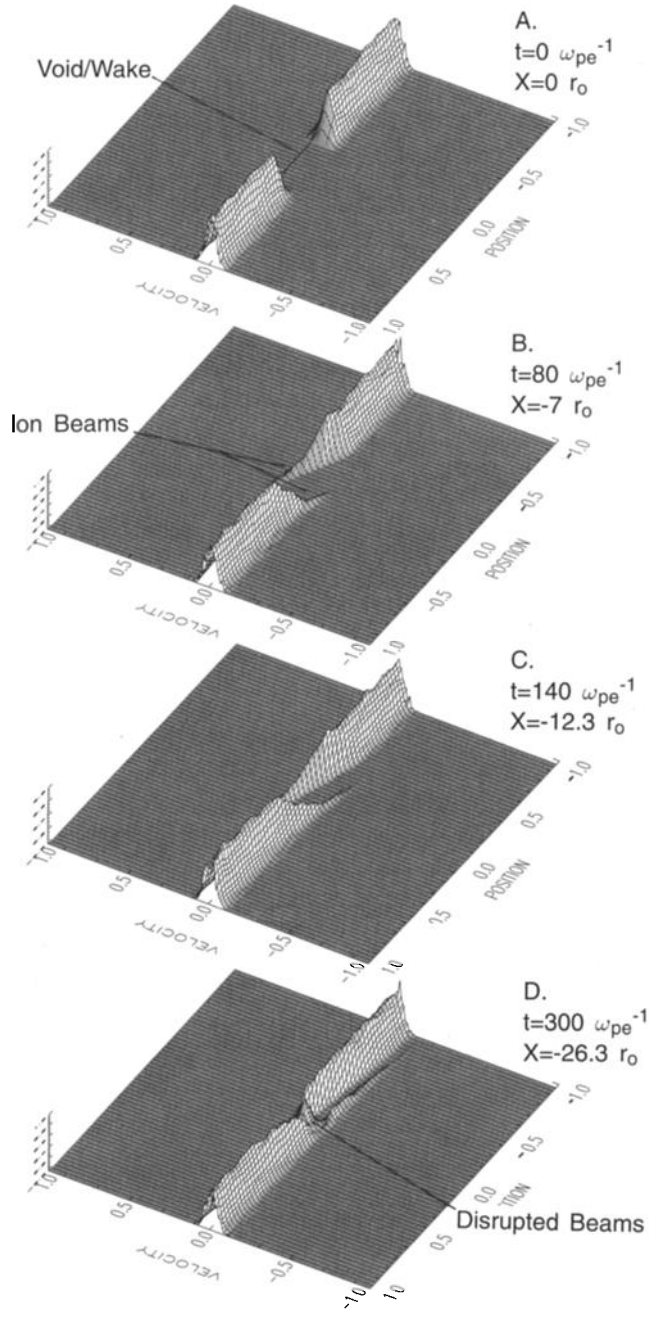

Figure 2. Ion velocity/configuration space distributions V_y versus Y) as a function of simulation time (and simulation distance down the tail).

2. A Description of a Simple Kinetic Simulation

The 1-D electrostatic particle-in-cell code uses 20,000 ions and electrons confined to a 500 Debye length space. The fields and particles are confined by periodic boundary conditions. In the central region, there is a void of missing particles of 125 Debye length that mimics a vacuum. The simulation is designed to monitor perpendicular forces and flows into the void, as a function of time. Again, the model is self-consistent and nonlinear process such as instabilities will also be observable in the simulation. The results of the simulation will then be compared to observations by particle, waves, and magnetic field instruments on Wind. A comparison the this self-consistent model can also be made to the analytical model presented by *Ogilvie et al.* [1996].

To compare this one-dimensional model to the lunar wake, we must also include effects from solar wind convection by the body. The solar wind is flowing past the absorbing disk at a speed v_{sw} of approximately 500 km/s. Consequently, there is a convection electric field present in the medium equal to $v_{sw}B$ sin θ_{vB}. However, we can always transform to a frame of reference where the electric field is zero. In this case, the reference frame is moving with the solar wind. The simulation presented here is run in a frame with background convection electric field removed, and is assumed to have each fluid element convecting tailward. Thus the one-dimensional particle

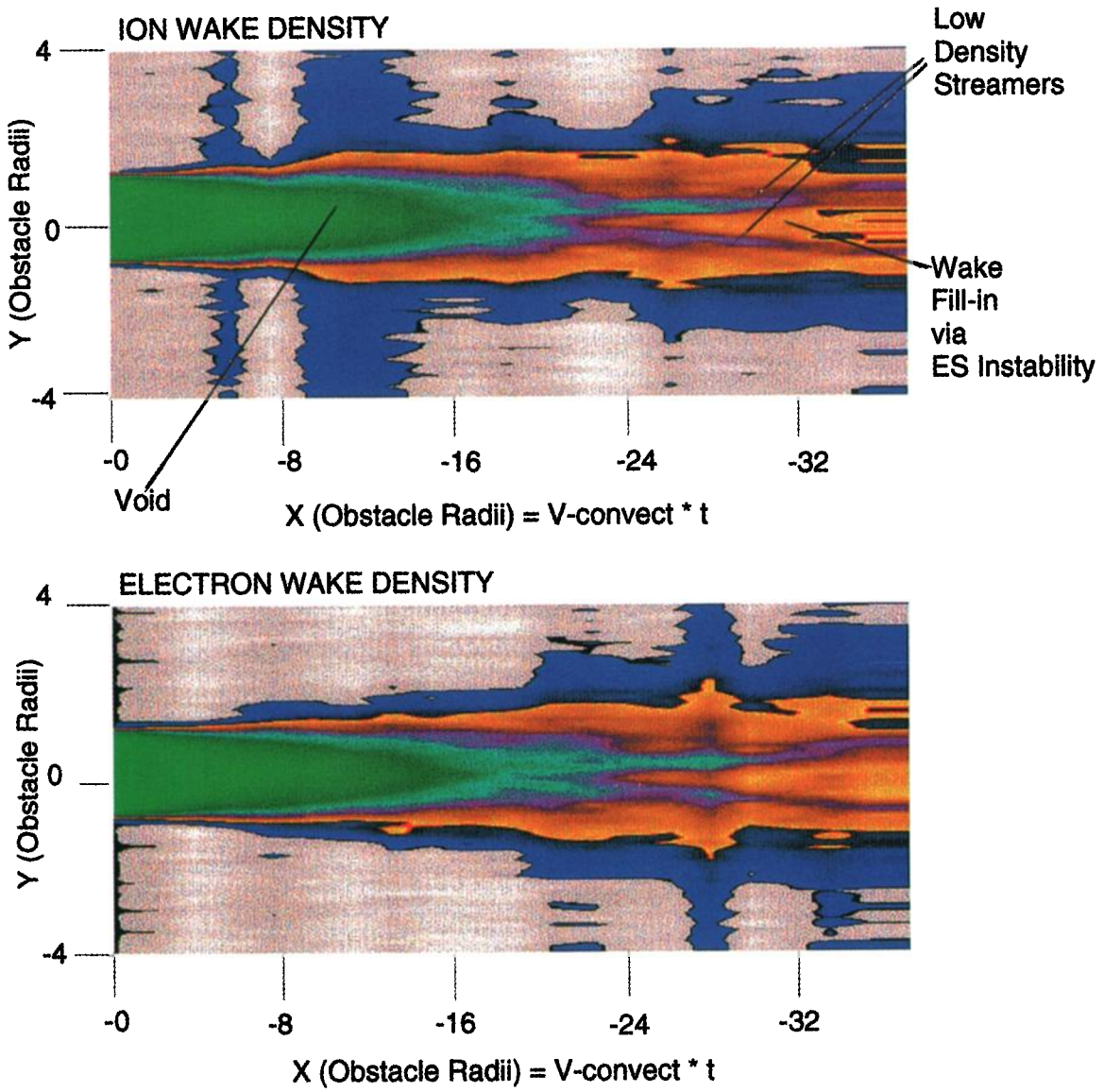

Plate 1. Ion and electron density.

simulation represents perpendicular forces and particle movements in a "slice" across the wake (in the Y direction, as indicated in Figure 1) which is moving tailward at $X = -V_{conv}t$. At $t = 0$, the distribution appears as it should immediately following lunar absorption. However, at a later time $t = t_0$, the electrodynamics is comparable to a location $X = -V_{conv}t_0$ along the wake tail. Inherent in the design of the simulation and the convection of the fluid slice discussed above is the assumption of a time-stationary lunar wake. In essence, as long as the ambient solar wind flow and interplanetary magnetic field remain constant, the wake morphology will remain spatially constant.

The 1-D ES 500 Debye length simulation is run for approximately 400 plasma periods. At this time, wake-accelerated ions and electrons leave the simulation box at the boundaries. Because the boundaries are periodic, these wake-accelerated particles will reappear at the opposite boundary as an anomalous and unphysical distribution. Thus the simulation must be terminated. To run the simulation for longer times, the dimension of the simulation space must be expanded.

3. Simulation Results

Figure 2 shows the ion configuration in V_y/Y (i.e., a cross-sectional "slice" across the wake) as a function of time. Note that at $t = 0$ there is an obvious and distinct void in the ion density, representing the initial placement of a wake or vacuum. After 80 plasma periods, we see the development of wakeward propagating ion beams from the flank regions, these moving inward toward the central wake region at velocities near the ion thermal speed. Near 300 plasma periods, electrostatic instabilities becomes significant, and cause the beams to distort in configuration space, leading to significant beam disruption. Note that wakeward ion beams [*Ogilvie et al.*, 1996] and corresponding electrostatic turbulence in the central wake [*Kellogg et al.*, 1996; *Bale et al.*, 1997; *Farrell et al.*, 1997] were observed by the Wind spacecraft.

Since the 1-D slice across the wake is also being "convected" down the tail as a function of time, the ion configuration evolving in time also represent the configurations at different locations along the wake tail (see Figure 1). The actual solar

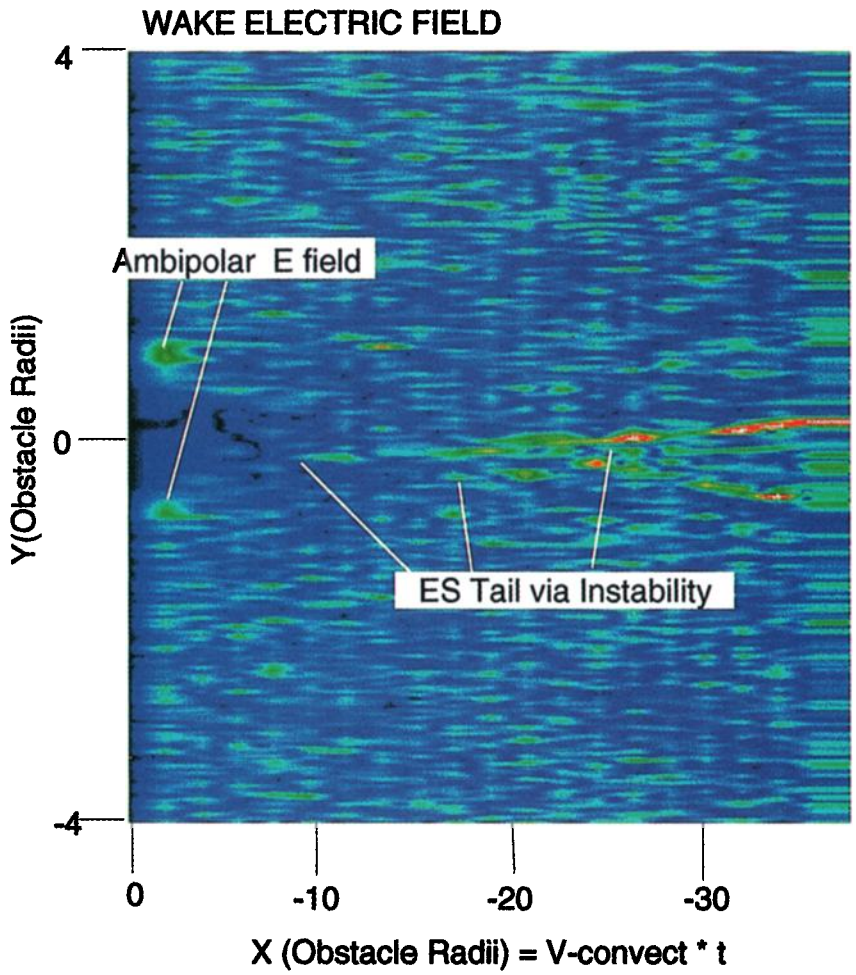

Plate 2. Wake electrostatic fields.

wind velocity, V_{sw}, is 25 times the ion thermal velocity v_{thi}. Thus, to simulate a similar flow, we require $X = -V_{conv}t$, where $V_{conv} = 25v_{thi}$ and t is measured in plasma periods, ω_{pe}^{-1}. The ion-to-electron mass ratio used in the simulation was 20, thereby making the electron thermal speed, $v_{the} \sim 4.5\ v_{thi}$. Using these parameters, we can convert the age of the slice to its location down the tail via the expression: $X = -8.75 \times 10^{-2} r_o t$, where t is in plasma periods and r_o is the radius of the of the simulated obstruction (in our case, $2r_o = 125$ simulation grids). For example, in Figure 2, the ion configuration after 300 ω_{pe}^{-1} is comparable to examining a wake "slice" at a location 26.2 r_o down the wake tail. The corresponding locations for each of the ion configurations shown in Figure 2 are labeled. The "slice" length we are examining is 500 λ_{De} or 8 r_o along the Y direction. Thus, making use of the scaling along X, we are able to map out the perpendicular flows and forces in an 8×35 obstacle radii region downstream of the obstacle.

Plate 1 shows the ion and electron density in the X/Y region downstream of the obstruction. The obstruction is located at $(X, Y) = (0, 0)$, has a width of $y = \pm 62.5$ simulation grids ($\pm 1 r_o$), and the solar wind is assumed to be incoming from the $+X$ direction. As evident in the figure, an obvious void in density of both species exists out to near $-16\ r_o$. Near $-20\ r_o$ the electrostatic instability in the central wake reaches appropriate strengths (i.e., transitions from linear growth to a saturated state) to cause disruption of the cross-tail ion beams (see Figure 2d). Consequently, the instability is capable of stopping the flow of beaming ions, thereby allowing them to be deposited in the central wake region. The result is to form a high-density region in the central wake (appearing like a "wedge") were beam disruption has occurred. On either side of the high-density region are low density "streamers" flaring outward from the wake tail. These regions have not yet been filled in by the instability process.

A density rarefaction wave traveling outward from the wake, back into the plasma, is also evident in Plate 1. This outward propagating wave forms due to the wakeward flow of plasma from the exterior region [*Ogilvie et al.*, 1996]. In order to replenish the wake, particles from adjacent regions are required. Upon examining the individual slices shown in Figure 2, it is clear that the wake edge becomes less defined, with ions instreaming from the external region. The extension of the disturbance into the external plasma defines the extent of the rarefaction wave. Since the wave travels outward near the ion sound speed, it is flared near 3° relative to the wake edges [*Ogilvie et al.*, 1996]. The simulation shows the rarefaction wave as the edges of the "blue" lower density region in Plate 1, which is also flared outward near 3°.

Plate 2 show the magnitude of the electric field in the X/Y region downstream of the obstruction. Note that the ambipolar electric field on the flanks of the wake (i.e., that drawing ions inward) is clearly evident, but extends only about 5 r_o behind the obstruction. It does not extend down the entire wake flank. This result suggests the ambipolar field does most of the par-

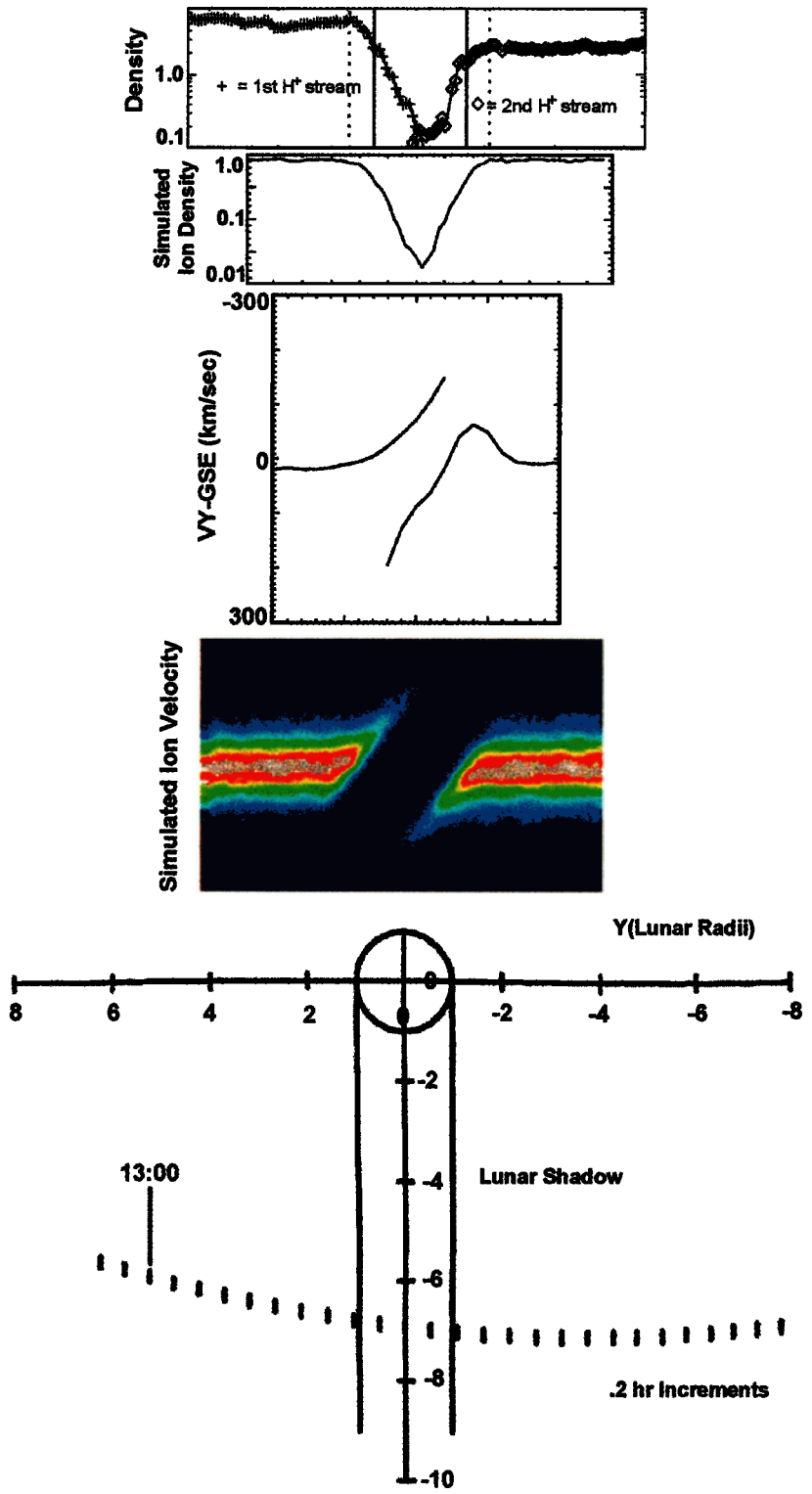

Plate 3. A comparison of measured and simulated ion properties for a cross-sectional transit near 7 obstacle radii.

ticle acceleration/beam formation relatively close to the obstruction. The beams, once formed, convects tailward. Near -7 r_o, the beams begin to feel their self-consistent electrostatic influence (i.e., commencement of the instability) in the central wake region.

As previously demonstrated, such counterstreaming beams are susceptible to an electrostatic instability [*Farrell et al.*, 1997], and much of the tail electric field between -7 and -37 r_o shown in the Plate 2 is a result of this mechanism. The simulation demonstrates that an electrostatic tail should form downstream of the obstruction, and is a time-stationary structure associated with the obstacle wake. The Wind spacecraft clearly observed this electrostatic tail on its passage through the lunar wake region [*Farrell et al.*, 1997; *Bale*, 1997]. Such an electrostatic structure could not be modeled (or predicted) via an MHD simulation [*Sprieter et al.*, 1970].

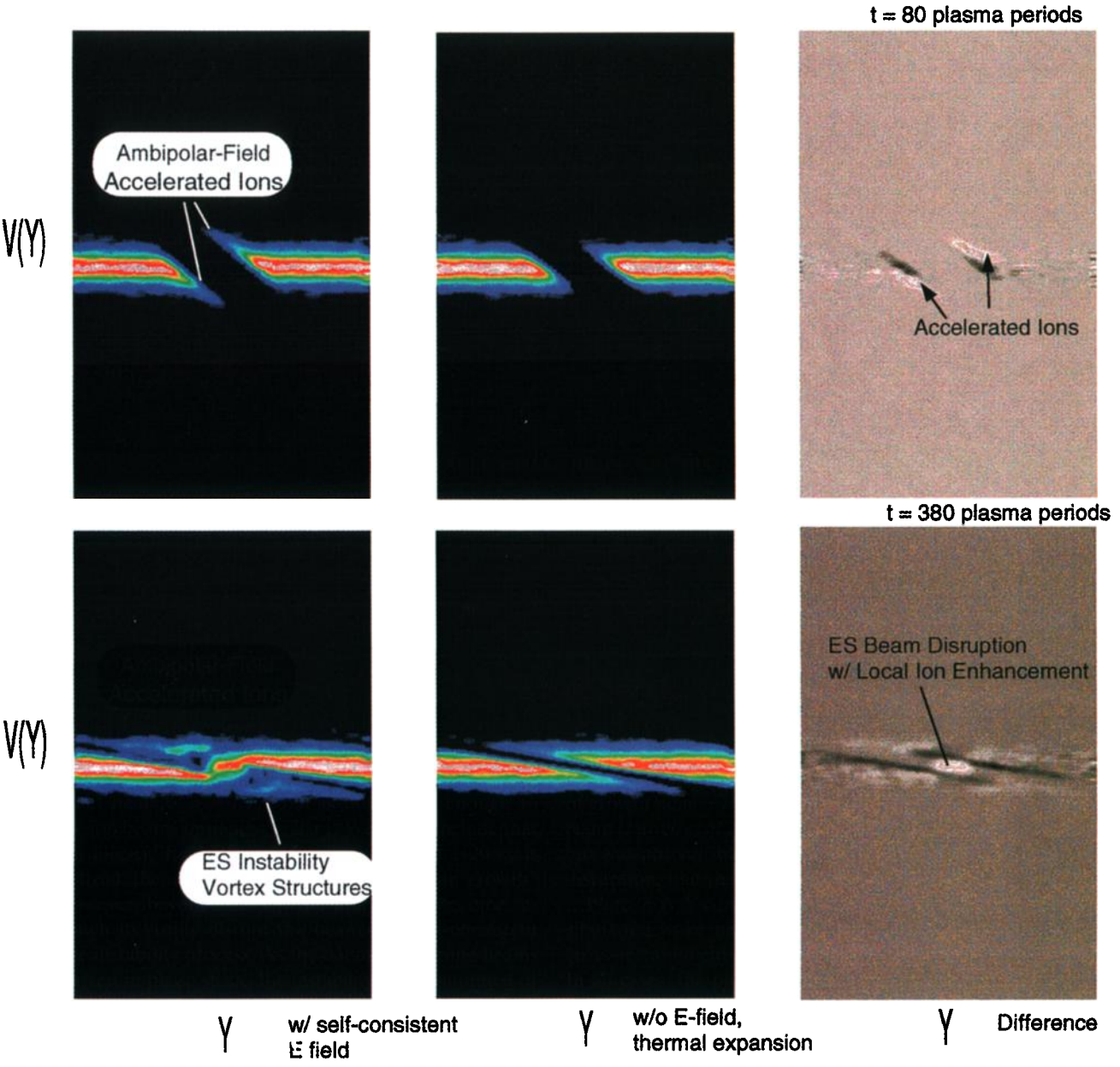

Plate 4. Electrostatic versus ballistic wake evolution. The top row displays the ion velocity distribution as a function of cross-wake position, Y. Shown is the simulated distribution including (left) electric forces, (middle) distribution from ballistic trajectories, and (right) their difference after 80 plasma periods. Note that an accelerated ion component is formed when electric forces are included. The bottom row displays the same distributions after the simulation has run for 380 plasma periods. Note that nonlinear structures, including a central density enhancement from beam disruption, forms when electrostatic forces are included.

We note that the electrostatic instability is observable in the electric field near $X = -7\ r_o$, but is not strong enough to disrupt the ion beams until near $-20\ r_o$. We thus conclude that the rise in electric field strength between -7 and $-20\ r_o$ is resulting from the instability being in the "linear growth" phase. However, beyond $-20\ r_o$, the amplitudes become intense enough to visibly disrupt the beam in a self-consistent way via the instability process. As the counterstreaming beams become mixed in phase space, the instability is in a saturated or "quenched" state.

This situation may explain the observations made by Wind during the December 27, 1994, lunar wake transit near $-7\ r_o$. The electrostatic instability was still in the early "linear" stages of growth near $-7\ r_o$ and thus did not substantially modify the beam [*Farrell et al.*, 1997]. Wave activity was observed by Wind, but was not yet intense enough to cause corresponding beam disruption, like that expected beyond $-20\ r_o$.

Plate 3 is a comparison of cross-sectional cuts across the simulated wake near the same region where Wind made its cross-sectional cut on December 24, 1994 (near $X = -7R_1$). In all cases, the plots were approximately scaled for comparison. The top two panels compare the Wind/SWE ion densities [*Ogilvie et al.*, 1996] to the simulated ion densities. Panel 3 and 4 shows a comparison of the ion cross-tail velocity component

(ion V_{Ygse}) as measured by Wind SWE (derived from *Ogilvie et al.* [1996]) to the contour of simulated ion velocity, V_y, as a function of Y near $X = -7\ r_o$. The simulation results are derived by taking cross-sectional "slices" across the wake near $X = -7\ r_o$. The bottom figure shows the Wind and wake geometry, at an appropriate scale to the measurements. Note that both the Wind and simulated densities are reduced by nearly 2 orders of magnitude in the central wake. The densities also vary exponentially (i.e., varies linearly when plotted logarithmically) to the local minimum. This situation is the hallmark of the ambipolar diffusion process [see *Ogilvie et al.*, 1996]. The Wind observations of ion cross-tail velocity shows counterstreaming ion beams in the central lunar wake, each beam moving in an opposite direction ($+Y$ and $-Y$) to the other and separated by 100–150 km/s. Each beam has a thermal speed of approximately 20 km/s, and the increased velocity of each beam (well above the thermal speed) as it moves toward the central wake is indicative of electrostatic acceleration (see Appendix). Note that the simulation shows the presence of the beams, as indicated in the fourth panel, this showing a contour plot of ions in $V_y - Y$ space. The measured ion beams show an increase in velocity (going from 2 to 4 times the thermal speed) as they move toward the central wake, and a nearly identical trend is present in the simulated beams. This ion beam acceleration is indicative of an underlying electrostatic force. The similarity in the measured and simulated results is quite remarkable.

4. Discussion and Conclusions

In the simulation, the magnetic field is assumed to lie along the Y axis, exactly perpendicular to the wake and parallel to the simulation particle velocity vector. Thus the results of the simulation are most applicable to a magnetic field geometry quasi-parallel to the Y-GSE direction. This set up aligns the expansion-related density gradient exactly along the ambient magnetic field. Further, given that the velocity vector is exactly parallel with the magnetic field direction, it is not necessary to include the magnetic field explicitly in the calculation. Obviously, given the limitations of the simulation, we cannot quantify the physics in cases where B is aligned along X-GSE (i.e., directed tailward).

With regard to the effects associated with the magnetic field direction, a fundamental question involves the orientation of the wake density gradient and ambipolar electric field with B field direction. Is this density gradient and ambipolar field primarily aligned along B, or is it primarily aligned perpendicular to the plasma flow direction (along Y-GSE)? The answer to this question actually involves the most basic understanding of the nature of the disturbance. Previously, the wake was considered primarily an MHD disturbance with magnetosonic wave structures characterizing the morphology [*Spreiter et al.*, 1970]. If this is truly the case, magnetic field orientation is critical for defining the angle of attack for wake-generated magnetosonic wave structures and the possible coupling of the disturbance to MHD modes. However, as described in section 2.3 of *Tidman and Krall* [1971], in a high beta plasma, ion sonic waves should be the dominate structures. In this latter case, the magnetic field orientation is of secondary importance as compared to the gradient in plasma density and flows. The new Wind observations of strong electrostatic turbulence and ion beam formation suggest a shift in paradigm from an MHD/magnetosonic wake to an ion sonic wake possessing an ion sonic outward rarefaction wave and an inward ion flow determined by the sonic speed, an ion flow that ultimately replenishes the wake. We thus suspect that the ambipolar electric field/density gradient will be aligned primarily perpendicular to the wake flank, along Y-GSE. The magnetic field will play some, but not a dominate, role in the interaction. However, to prove this hypothesis explicitly, a higher-dimension simulation is required, and/or a systematic observational survey is required of all the Wind passes through the wake region under varying IMF orientations.

The simulation does suffer from some other obvious limitations. For example, the forces and flows parallel to the wake (i.e., the X direction) are not considered. Consequently, diamagnetic currents like those suggested by *Owen et al.* [1996] are not modeled. Also, waves generated at oblique angles (i.e., with a wave vector component in the X direction) are not simulated. Consequently, upstream "precursor" whistler waves [*Farrell et al.*, 1996] and whistler "wings" [*Gurnett et al.*, 1995a, b] cannot be modeled. Further, the electron wings observed by Wind and modeled by *Bale* [1997] are not recreated in this model, again possibly due to the limitation of movement to one explicit dimension. Specifically, if the upstream disturbances are realted to an oblique electromagnetic wave moving ahead of the wake, they will no be modeled in this 1-D electrostatic simulation.

Despite these drawbacks, a kinetic model of the lunar wake dynamics can successfully explain the observed elongated wake and associated ion dynamics in the central region. MHD simulations [*Spreiter et al.*, 1970] suggest the lunar wake fills-in ~3–5 lunar radii, with the subsequent development of a trailing shock. In contrast, the kinetic model suggests a longer wake, this replenishing via an ion beam flow and electrostatic instability. This instability also creates a long central tail of electrostatic turbulence. This electrostatic tail is a direct byproduct of replenishing the wake, and represents the stimulated electrostatic phonons released in slowing (or "braking") the inflowing ions. This electrostatic activity might be considered "electrostatic bremsstrahlung," implying that the electrostatic waves are directly associated with the process of decelerating the ion beams.

In a historical context, in the late 1960s, some discussion occurred between Y. C. Whang and J. R. Spreiter on the nature of the lunar wake, and its treatment in a particle or fluid context. This discussion is cited in a fair presentation by *Spreiter et al.* [1970]. The Wind observations and associated studies have aided in obtaining a further understanding of the dominate processes, suggesting that particle dynamics plays a role that was previously unappreciated. We conclude that the physics of the lunar wake is very different from that previously presented in a standalone MHD formalism, with electrostatic processes acting in a major role to replenish the plasma void.

We thus suggest that the variable of merit in defining the lunar wake may not be the magnetosonic speed, but instead the ion sonic speed. *Tidman and Krall* [1971] indicate a preference for ion sonic disturbances over magnetosonic disturbances in a high-beta plasma. The magnetic field, frozen in, is then simply responding to the modification of the plasma. In the case of the lunar wake, it is the ion beams that ultimately fill in the void, and their beam speed at 1/20 the solar wind convection speed implies a flank convergence behind the body at ~20–30 R_L. This result is very different from the 4–5 R_L predicted by MHD simulation [*Spreiter et al.*, 1970]. We suspect that the emphasis on a magnetosonic wake revolves around the lack of

microphysical data obtained via Explorer 35 and Apollo subsatellite missions in the early 1970s. However, the modern instrumentation onboard Wind has detected a lunar wake far more kinetic than originally appreciated.

Appendix: Comparison With Neutral Thermal Expansion Into a Void

As an exercise, we compare the plasma thermal expansion into a vacuum to that of neutral thermal expansion to determine similarities and differences in the two processes. To simulate a neutral environment, we modeled a two particle gas having the same thermal distribution and mass as the charged case described in the text above. However, we set all electric force terms to zero. Thus particle velocities are unaltered during the course of the simulation run; trajectories being simply "ballistic" in nature.

Plate 4 is a comparison of the two scenarios. Shown is the ion velocity distribution, $F(y, v_y, E, t)$ in velocity/configuration $v_y - y$ space. The panels in the far left columns show the ion distribution for the electrostatic PIC code with electric forces. The panels in the middle column show the distributions with no electric forces (i.e., ballistic trajectories). The panels in the far right column represent the difference between the two distributions, $F(y, v_y, E, t) - F(y, v_y, E = 0, t)$.

The top row compares distributions and their differences after 80 plasma periods. In both cases, ion beams begin to form due to the finite spread of the initial distribution. However, with the inclusion of the electric field in the ES PIC code, an additional accelerated component to the ion distribution is formed having velocities greater than the ballistic case. The velocities exceed those of the initial distribution by a factor of 2–3, and progressively increase from the wake edge inward toward the central region. This accelerated component is identified in Plate 4. The acceleration results from the ambipolar electric field at the wake edge (which is not modeled in the ballistic case). Because of their increased velocity, the ambipolar-accelerated ions fill in the void quicker than simple ballistic ions.

At 380 plasma periods, the thermal evolution of the ballistic particles shown in the lower, middle panel form two uninterrupted beams in the central wake region. However, the ions beams under the influence of the self-consistent electrostatic field are disrupted due to an electrostatic instability [*Farrell et al.*, 1997]. As a result, a central ion density enhancement appears due to the effect of the instability-related fields. In regions adjacent to the central density enhancement, beam deceleration is present with beam velocities quickly changing from $v = 2$–$3\ v_{th_i}$ to $v = 0$. Secondary beams associated with outward propagating vortex structures also appear, rolling and flowing in the classic "waterbag" style toward the simulation box edges.

Thus thermal dispersion creates ion beam formation into the wake, but the accelerated component observed above the thermal speed, like that in Figure 1 of *Ogilvie et al.* [1996] and redisplayed here in Plate 3 is associated with the added ambipolar electric field that forces ions into the wake region. This field accelerates wake replenishment by pushing ions to the central region faster than the ballistic case. The electrostatic instability appears to then disrupt the beams, creating a buildup of ions in the central wake region.

References

Bale, S. D., Shadowed particle distributions near the Moon, *Geophys. Res. Lett.*, *102*, 19,773, 1997.

Bale, S. D., et al., Evidence of currents and unstable particle distributions extended around the lunar plasma wake, *Geophys. Res. Lett.*, *24*, 1427, 1997.

Bosqued, J. M., et al., Moon-solar wind interaction: First results from the WIND/3DP experiment, *Geophys. Res. Lett.*, *23*, 1259, 1996.

Bougeret, J.-L., et al., The radio and plasma wave investigation on the WIND spacecraft, *Space Sci. Rev.*, *71*, 231, 1995.

Farrell, W. M., et al., Upstream ULF waves and energetic electrons associated with the lunar wake: Detection of precursor activity. *Geophys. Res. Lett.*, *23*, 1271, 1996.

Farrell, W. M., M. L. Kaiser, and J. T. Steinberg, Electrostatic instability in the central lunar wake: A process for replenishing the plasma void? *Geophys. Res. Lett.*, *24*, 1135, 1997.

Gurnett, D. A., The whistler-mode bow wave of an asteroid, *J. Geophys. Res.*, *100*, 21623, 1995a.

Gurnett, D. A., On the remarkable similarity between the propagation of whistlers and the bow wave of a ship, *Geophys. Res. Lett.*, *22*, 1865, 1995b.

Kellogg, P. J., et al., Observations of plasma waves during a traversal of the moon's wake, *Geophys. Res. Lett.*, *23*, 1267, 1996.

Lepping, R. P., et al., The WIND magnetic field investigations, *Space Sci. Rev.*, *71*, 207, 1995.

Ogilvie, K. W., et al., SWE, a comprehensive plasma instrument for the WIND spacecraft, *Space Sci. Rev.*, *71*, 55, 1995.

Ogilvie K. W., et al., Observations of the lunar plasma wake from hte WIND spacecraft on December 27 1994, *Geophys. Res. Lett.*, *23*, 1255, 1996.

Owen, C. J., et al., The lunar wake at 6.8 R1: WIND magnetic field observations, *Geophys. Res. Lett.*, *23*, 1263, 1996.

Samir, U, K. H. Wright Jr., N. H. Stone, The expansion of plasma into a vacuum: Basic phenomena and processes and applications to space plasma physics, *Rev. Geophys.*, *21*, 1631, 1983.

Spreiter, J. R., M. C. Marsh, and A. L. Summers, Hydromagnetic aspects of solar wind flow past the moon, *Cosmic Electrodyn.*, *1*, 5, 1970.

Tidman, D. A., and N. A. Krall, *Shock Waves in Collisionless Plasmas*. John Wiley, New York, 1971.

S. D. Bale, Space Science Laboratory, University of California, Berkeley, CA 94720.

W. M. Farrell and M. L. Kaiser, Laboratory for Extraterrestrial Physics, NASA Goddard Space Flight Center, Greenbelt, MD 20771.

J. T. Steinberg, Center for Space Research, Massachusetts Institute of Technology, Cambridge, MA 02139.

(Received July 14, 1997; revised November 7, 1997;
accepted December 18, 1997.)